Transport Properties of Aqueous Solutions of (1*R*,2*S*)-(−)- and (1*S*,2*R*)-(+)-Ephedrine Hydrochloride at Different Temperatures

Artur J. M. Valente,*,† Ana. C. F. Ribeiro,† Jorge M. C. Marques,† Paulo E. Abreu,† Victor M. M. Lobo,† and Ritu Kataky‡

Department of Chemistry, University of Coimbra, 3004-535 Coimbra, Portugal, and Department of Chemistry, University of Durham, Durham, DH1 3LE, U.K.

Electrical conductivity and mutual diffusion coefficients of aqueous solutions of two ephedrine enantiomers ((1*S*,2*R*)-(+)-ephedrine hydrochloride and (1*R*,2*S*)-(−)-ephedrine hydrochloride), at a concentration range of (0 to 0.17) mol·dm^{-3} and (0.001 to 0.01) mol·dm^{-3}, respectively) have been measured. The effect of temperature, ranging from (298.15 to 323.15) K, has also been studied. The experimental data of electrical conductivity follow the Kohlrausch equation, and the hydration radius of ephedrines can be calculated from Walden rule equation. The activation enthalpies of the transport process for ephedrine cations, (1*R*,2*S*)-(−)-ephedrine and (1*S*,2*R*)-(+)-ephedrine, 7.4 (± 0.5) kJ·mol^{-1} and 19.3 (± 0.4) kJ·mol^{-1}, respectively, show a slight discrimination between both enantiomers. The experimental data are discussed on the basis of the Onsager−Fuoss model. The Nernst diffusion coefficients for (1*R*,2*S*)-(−)- and (1*S*,2*R*)-(+)-ephedrine hydrochloride in water, at (298.15 and 310.15) K, derived from conductance and from diffusion experiments are in good agreement.

1. Introduction

Ephedrine is an alkaloid extract from *Ephedra* or Ma Huang (*Ephedra sinica*) species. Ephedrine and ephedrine derivatives (e.g., methylephedrine and norephedrine) are sympathomimetic amines known to have central nervous system stimulating properties,[1] producing excitement and euphoria and increasing motor activity,[2] which has direct effects on the regulations of the World Anti-Doping Agency (WADA). However, ephedrines are also used as a major active component in medications for the treatment of nasal congestion,[3] asthma, and obesity.[4] As a consequence of a widespread use of ephedrine, it has been necessary to develop analytical techniques for their reliable detection, including different hyphenated techniques, such as gas chromatography/mass spectrometry,[5] gas chromatography/electron ionization mass spectrometry,[6] and liquid chromatography/mass spectrometry/mass spectrometry.[7] Another important characteristic of ephedrines is the existence on their structure of two chiral centers, with the corresponding four isomers: (1*S*,2*R*)-(+)-ephedrine, (1*R*,2*S*)-(−)-ephedrine, (1*S*,2*S*)-(+)-pseudoephedrine, and (1*R*,2*R*)-(−)-pseudoephedrine.[8] These chiral properties make ephedrine an interesting model for the development of sensors[9−11] and molecular imprinted polymers for chiral recognition.[12−15] Despite the above-mentioned applications of ephedrines, no information on transport properties of these compounds is available.

Transport properties, such as electrical conductivity and diffusion coefficients, will help to better understand the structure of drug−solvent and drug−drug interactions in aqueous solutions[16−19] and thus contribute to the development and analysis of the behavior of ephedrine in the biological fluids, where water is the major solvent, as well as for the development of new sensors.

Scheme 1

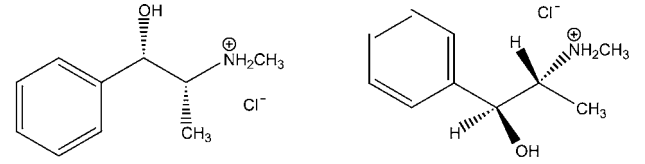

(1R,2S)-(-)-ephedrine hydrochloride (1S,2R)-(+)-ephedrine hydrochloride

In the present work, electrical conductances and mutual diffusion coefficients (*D*) of aqueous solutions of (+)- and (−)-ephedrine, at the temperatures from (283.15 to 323.15) K and (298.15 and 310.15) K, respectively, are reported. Molecular dynamic simulations of ephedrine enantiomers will help to establish a relationship between the experimental data and the structure of solutions.

From the experimental results of conductivities and from the mean distance of closest approach, computed from molecular dynamic simulations (MDS's), diffusion coefficients of ephedrines, by using the Onsager−Fuoss model, are estimated and compared with experimental *D* values.

2. Experimental Section

2.1. Materials. (1*R*,2*S*)-(−)-Ephedrine hydrochloride (99 %) and (1*S*,2*R*)-(+)-ephedrine hydrochloride (99 %), Scheme 1, were purchased from Sigma-Aldrich and were used without further purification. The solutions for the conductivity and diffusion measurements were prepared in calibrated volumetric flasks using Millipore-Q water. The solute was weighed using a Scaltec SBC22 balance with a resolution of ± 0.00001 g.

2.2. Electrical Conductance Measurements. Solution electrical resistances were measured with a Wayne-Kerr model 4265 automatic LCR meter at 1 kHz. A Shedlovsky type conductance

* Corresponding author. Phone: +351 239854459. Fax: +351 239 827703. E-mail: avalente@ci.uc.pt.
† University of Coimbra.
‡ University of Durham.

10.1021/je9005757
Published on Web 09/21/2009

cell, with a cell constant of 0.1002 cm^{-1}, was used.[20] Cell constants were determined from measurements with KCl (reagent grade, recrystallized, and dried) using the procedure and data of Barthel et al.[21] Measurements were taken at temperatures ranging from (283.15 to 323.15) K (± 0.02 K) in a HAAKE Phoenix II P2 thermostat bath. Solutions were always used within 12 h of preparation. In a typical experiment, 20.0 mL of water was placed in the conductivity cell; then, aliquots of the ephedrine solutions were added in a stepwise manner using a Metrohm 765 Dosimate micropipet. The conductance of the solution was measured after each addition and corresponds to the average of three ionic conductances (with the uncertainty less than 0.2 %).[22] The time necessary to obtain the thermostatic equilibrium and the corresponding electrical resistance values is controlled through homemade software.

2.3. Mutual Diffusion Coefficient Measurements. An open-ended capillary cell, which has been used to obtain mutual diffusion coefficients for a wide variety of electrolytes, is described in great detail in previous papers.[23−27] Basically, this consists of two vertical capillaries each closed at one end by a platinum electrode and positioned one above the other with the open ends separated by a distance of about 14 mm. The upper and lower tubes, initially filled with solutions of concentrations of 0.75*c* and 1.25*c*, respectively, are surrounded with a solution of concentration *c*. This ambient solution is contained in a glass tank, (200 × 140 × 60) mm, immersed in a thermostat bath at 25 °C. Perspex sheets divide the tank internally, and a glass stirrer creates a slow lateral flow of ambient solution across the open ends of the capillaries. Experimental conditions are such that the concentration at each of the open ends is equal to the ambient solution value *c*; that is, the physical length of the capillary tube coincides with the diffusion path. This means that the required boundary conditions described in the literature to solve Fick's second law of diffusion are applicable. Therefore, the so-called Δl effect is reduced to negligible proportions. In our manually operated apparatus, diffusion is followed by measuring the ratio $w = R_t/R_b$ of resistances R_t and R_b of the upper and lower tubes by an alternating current transformer bridge. In our automatic apparatus, *w* is measured by a Solartron digital voltmeter (DVM) 7061 with 6 1/2 digits. A power source (Bradley Electronic model 232) supplies a 30 V sinusoidal signal at 4 kHz (stable to within 0.1 mV) to a potential divider that applies a 250 mV signal to the platinum electrodes in the top and bottom capillaries. By measuring the voltages V′ and V″ from top and bottom electrodes to a central electrode at ground potential in a fraction of a second, the DVM calculates *w*.

To measure the differential diffusion coefficient *D* at a given concentration *c*, the bulk solution of concentration *c* is prepared by mixing 1 L of "top" solution with 1 L of "bottom" solution, measured accurately. The glass tank and the two capillaries are filled with *c* solution, immersed in the thermostat, and allowed to come to thermal equilibrium. The resistance ratio $w = w_\infty$ measured under these conditions (with solutions in both capillaries at concentration *c*) accurately gives the quantity $\tau_\infty = 10^4/(1 + w_\infty)$.

The capillaries are filled with the "top" and "bottom" solutions, which are then allowed to diffuse into the "bulk" solution. Resistance ratio readings are taken at various recorded times, beginning 1000 min after the start of the experiment, to determine the quantity $\tau = 10^4/(1 + w)$ as τ approaches τ_∞. The diffusion coefficient is evaluated using a linear least-squares procedure to fit the data, and finally, an iterative process is applied using 20 terms of the expansion series of Fick's second law for the present boundary conditions. The theory developed for the cell has been described elsewhere.[23]

2.4. Molecular Dynamics Simulations (MDS's). An MDS for both (1*R*,2*S*)-(−)- and (1*S*,2*R*)-(+)-ephedrine isomers surrounded, respectively, by 2989 and 3004 water molecules at $T = 298.15$ K and $T = 310.15$ K has been performed. Since the ephedrine is expected to be in its ionic form, the Cl^- counterion was added to the solution. All of the simulations have used the GROMACS package,[28] while the force field was built as follows: (i) the Topolbuild program (version 1.2.1) was employed to generate the ephedrine topology within the generalized assisted model building with energy refinement (AMBER) force field (so-called GAFF[29]); (ii) charges in the atoms were calculated at the HF/6-31G* level of theory, according to the usual procedure for the AMBER force field;[30−33] (iii) then, the water molecules and the counterion were added to fulfill the simulation box; (iv) the SPC/E (extended simple point charge model) potential[34,35] has been used for the water molecules.

The simulations were carried out in a cubic box (∼$45 \cdot 10^{-10}$ m per edge) with periodic boundary conditions and a cutoff radius of $15 \cdot 10^{-10}$ m ($12 \cdot 10^{-10}$ m) for Coulomb (van der Waals) interactions; the density of the solution is fixed at 0.99 $g \cdot cm^{-3}$. After an initial energy minimization, the equations of motion were integrated with a step of 1 fs during a total of 4400 ps; the first 23 % of the trajectory is assumed as the equilibration part of the simulation, and hence, the analysis was performed only over the last 3400 ps (i.e., the production part). The average temperature was kept constant by coupling the system with a Nosé-Hoover thermostat[36] (with the period τ_T of the oscillations of kinetic energy between the system and the reservoir of 1 ps).

From the present simulations, we have obtained the mean distance of closest approach of ephedrine hydrochloride. Another important structural quantity that has been extracted from the MDS is the radial distribution function (RDF); this is particularly important to get insight about the structure of the water surrounding the ephedrine species.

3. Experimental Results and Discussion

3.1. Electrical Conductivities. The molar conductivities, Λ, of (1*R*,2*S*)-(−)-ephedrine hydrochloride, (−)-eph, and (1*S*,2*R*)-(+)-ephedrine hydrochloride, (+)-eph, are calculated using

$$\Lambda = \frac{(\kappa - \kappa_0) \cdot 1000}{c} \tag{1}$$

where κ and κ_0 are the specific electrical conductances, in $S \cdot cm^{-1}$, of ephedrine aqueous solution and solvent, respectively, and *c* is the molar concentration in $mol \cdot dm^{-3}$. Tables 1 and 2 show the molar conductivities of (−)-eph and (+)-eph, respectively, at different temperatures ranging from 283.15 to 323.15 K.

The molar conductivity data show a linear relationship, in the concentration range (1.84 to 16.67)$\cdot 10^{-3}$ $mol \cdot dm^{-3}$, with the square root of concentration of ephedrine, in agreement with the Kohlrausch equation[37]

$$\Lambda = \Lambda^0 - A \cdot c^{1/2} \tag{2}$$

where Λ^0 is the molar conductivity at infinite dilution of ephedrine hydrochloride and *A* is a function of the dielectric constant and viscosity of the medium, temperature, and the radius of the "ionic atmosphere". The fitting parameters of experimental data of Λ to eq 2, for both ephedrine hydrochloride enantiomers and temperatures, are reported in Table 3. These parameters were obtained by a least-squares linear regression method using Origin 7.5 software taking 95 % confidence limits. From the analysis of data shown in Tables 1 to 3, it is possible

Table 1. Molar Conductivities, Λ, of (1*R*,2*S*)-(−)-Ephedrine Hydrochloride in Aqueous Solutions at Different Temperatures

T/K	283.15	293.15	298.15	303.15	310.15	323.15
$10^3 \cdot c^a$	Λ/S·cm²·mol⁻¹					
1.840	65.71	83.75	94.63	104.10	119.48	149.54
2.438	64.63	81.98	92.82	102.27	117.29	147.08
3.030	63.55	80.59	91.27	100.62	115.37	144.87
3.614	62.80	79.07	89.91	99.14	113.90	142.73
4.191	61.81	77.75	88.60	98.02	112.54	140.79
4.761	61.03	76.63	87.53	96.63	110.78	139.17
5.324	60.44	75.64	86.53	95.67	109.64	137.66
5.881	59.90	74.68	85.56	94.74	108.51	135.63
6.431	59.25	73.77	84.65	93.63	107.44	134.40
6.975	58.60	72.88	83.74	92.71	106.35	133.15
7.513	57.94	71.99	82.83	91.97	105.24	131.84
8.044	57.36	71.19	81.99	91.10	104.22	130.66
8.569	56.85	70.44	81.20	90.28	103.26	129.54
9.089	56.35	69.74	80.44	89.49	102.34	128.44
9.602	55.84	69.08	79.75	88.78	101.49	127.43
10.110	55.37	68.46	79.08	88.07	100.66	126.43
10.612	54.91	67.95	78.40	87.34	99.82	125.40
11.108	54.46	67.23	77.74	86.65	99.01	124.40
11.599	54.01	66.63	77.09	85.96	98.21	123.42
12.085	53.59	66.04	76.46	85.28	97.42	122.56
12.565	53.20	65.49	75.86	84.64	96.73	121.50
13.040	52.81	64.98	75.30	84.37	96.02	120.62
13.510	52.44	64.48	74.74	83.43	95.33	119.73
13.975	52.10	64.00	74.22	82.86	94.67	118.90
14.435	51.76	63.54	73.70	82.30	94.01	118.08
14.890	51.40	63.07	73.18	81.74	93.36	117.25
15.340	51.07	62.60	72.67	81.18	92.71	116.44
15.786	50.75	62.17	72.17	80.64	92.08	115.64
16.226	50.42	61.74	71.70	80.12	91.46	114.86
16.663	50.11	61.33	71.25	79.62	90.88	114.11

[a] Units: c, mol·dm⁻³.

Table 2. Molar Conductivities, Λ, of (1*S*,2*R*)-(+)-Ephedrine Hydrochloride in Aqueous Solutions at Different Temperatures

T/K	283.15	293.15	298.15	303.15	310.15	323.15
$10^3 \cdot c^a$	Λ/S·cm²·mol⁻¹					
1.841	65.45	84.40	93.66	104.07	120.09	152.45
2.440	64.22	82.68	91.79	102.01	117.74	148.94
3.031	63.16	81.09	90.34	100.08	115.90	146.93
3.615	62.04	79.73	89.01	98.37	114.06	144.37
4.193	61.01	78.49	87.78	97.03	112.20	142.24
4.763	60.18	77.49	86.75	95.66	110.67	140.14
5.327	59.42	76.61	85.77	94.39	109.39	138.41
5.884	58.66	75.70	84.81	93.20	107.94	136.77
6.434	57.95	74.86	83.90	92.08	106.97	135.19
6.978	57.25	73.95	82.98	90.99	105.72	133.68
7.516	56.55	73.10	82.05	89.91	104.63	132.16
8.048	55.93	72.32	81.20	88.93	103.63	130.78
8.573	55.34	71.59	80.40	88.00	102.67	129.48
9.093	54.77	70.89	79.65	87.13	101.75	128.27
9.607	54.27	70.27	78.96	86.33	100.90	127.11
10.115	53.77	69.66	78.29	85.56	100.08	126.01
10.617	53.29	69.04	77.61	84.78	99.23	124.90
11.114	52.84	68.44	76.95	84.04	98.41	123.84
11.605	52.42	67.85	76.30	83.29	97.60	122.78
12.091	51.96	67.29	75.67	82.57	96.79	121.74
12.571	51.56	66.75	75.01	81.90	96.03	120.76
13.046	51.18	66.26	74.50	81.26	95.32	119.84
13.517	50.78	65.76	73.95	80.64	94.61	118.94
13.982	50.38	65.28	73.43	80.05	93.94	118.09
14.442	50.03	64.83	72.91	79.46	93.28	117.23
14.897	49.66	64.37	72.39	78.88	92.61	116.38
15.347	49.29	63.90	71.88	78.31	91.96	115.54
15.793	48.94	63.43	71.38	77.76	91.32	114.73
16.234	48.61	63.02	70.90	77.22	90.69	113.93
16.670	48.32	62.62	70.45	76.71	90.10	113.18

[a] Units: c, mol·dm⁻³.

to conclude that ephedrine enantiomers behave, in the concentration range analyzed, as strong electrolytes. The molar conductivities at infinitesimal concentrations are estimated with an uncertainty lower than 0.095 %.

Table 3. Molar Limiting Conductivities, Λ^0, of Ephedrines Calculated from Fitting the Experimental Data, Shown in Tables 1 and 2, to Equation 3

	T / K	Λ^0 (± s)[a] S·cm²·mol⁻¹	$A \cdot 10^{-3}$ S·mol$^{-3/2}$·cm$^{7/2}$	R^{2b}
(−)-eph⁺	283.15	73.71 (± 0.06)	5.77 (± 0.02)	0.9997
	293.15	94.62 (± 0.09)	8.20 (± 0.03)	0.9996
	298.15	106.26 (± 0.09)	8.57 (± 0.01)	0.9999
	303.15	116.31 (± 0.09)	8.94 (± 0.03)	0.9997
	310.15	133.82 (± 0.09)	10.47 (± 0.03)	0.9998
	323.15	167.4 (± 0.1)	12.98 (± 0.03)	0.9997
(+)-eph⁺	283.15	73.98 (± 0.06)	6.32 (± 0.02)	0.9996
	293.15	94.90 (± 0.06)	7.93 (± 0.02)	0.9998
	298.15	105.31 (± 0.07)	8.52 (± 0.02)	0.9998
	303.15	117.52 (± 0.07)	10.31 (± 0.02)	0.9999
	310.15	134.68 (± 0.08)	10.91 (± 0.03)	0.9999
	323.15	171.51 (± 0.09)	14.30 (± 0.03)	0.9999

[a] s: standard deviation. [b] R^2: correlation coefficient.

Table 4. Limiting Ionic Conductivities of Chloride and Ephedrine Ions at Different Temperatures

		(−)-eph⁺		(+)-eph⁺	
T / K	$\lambda^0(Cl^-)$ S·cm²·mol⁻¹	λ^0 S·cm²·mol⁻¹	r_h 10^{-9}·m	λ^0 S·cm²·mol⁻¹	r_h 10^{-9}·m
283.15	54.28	19.43 (± 0.06)	0.322	19.00 (± 0.02)	0.329
293.15	68.75	25.87 (± 0.09)	0.316	26.15 (± 0.06)	0.313
298.15	76.35	29.91 (± 0.04)	0.308	28.96 (± 0.09)	0.318
303.15	84.18	32.13 (± 0.09)	0.319	33.34 (± 0.08)	0.307
310.15	95.52	38.30 (± 0.09)	0.307	39.16 (± 0.09)	0.300
323.15	117.65	49.75 (± 0.09)	0.293	53.86 (± 0.09)	0.279

From molar conductivities at infinitesimal concentration Λ^0 (Tables 1 and 2), the limiting ionic conductivity of the cationic ephedrines ($\lambda^0(eph^+)$) can be calculated through eq 3

$$\Lambda^0 = \lambda^0(eph^+) + \lambda^0(C1^-) \quad (3)$$

where the limiting ionic conductivity of chloride ions, $\lambda^0(Cl^-)$, were obtained from the eq 4[38]

$$\lambda^0(Cl^-)_t = \lambda^0(Cl^-)_{25} + \alpha(t - 25) + \beta(t - 25)^2 + \gamma(t - 25)^3 \quad (4)$$

where t is the temperature in Celsius degrees, $\lambda^0(Cl^-)_{25}$ is equal to 76.35 S·cm²·mol⁻¹, and α, β, and γ are constants with the following values: 1.54037 S·cm²·mol⁻¹·°C⁻¹, 0.46500·10⁻⁴ S·cm²·mol⁻¹·°C⁻², and −0.1285·10⁻⁴ S·cm²·mol⁻¹·°C⁻³, respectively. The values obtained for $\lambda^0(eph^+)$ and $\lambda^0(Cl^-)$, at different temperatures, are reported in Table 4. In general, it is possible to conclude that the ionic conductivities of both enantiomers are quite similar; however, it seems that by increasing the temperature ($T > 298.15$ K) the ionic conductivities of (+)-eph⁺ become higher, even if only by around 4 %, than the corresponding values for (−)-eph⁺ (Figure 1). This conclusion is also supported by a slight difference in the activation enthalpy for transport process: see the discussion below. Studies on the electrical conductance of solutions are related to the investigation of solvation and electrotransport properties of the constituent ions. These properties depend on both the ionic radius and the degree of ionic hydration.[39] Consequently, to have a deeper insight on the factors affecting the transport mechanism, we have calculated the hydrodynamic radii (r_h) for both ephedrine ions and its dependence on temperature, using the equation[16,40]

$$\lambda^0 = \frac{F \cdot e \cdot |z|}{6 \cdot \pi \cdot \eta^0 \cdot r_h} \quad (5)$$

where F is the Faraday constant, e is the elementary charge, and z is the ionic charge. The values of r_h, listed in Table 4,

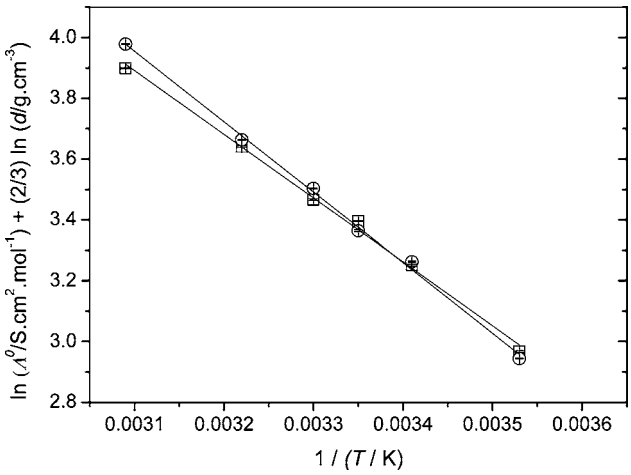

Figure 1. Dependence of the natural logarithm molar conductivity at infinitesimal concentration, with a solvent density correction, on the reverse of temperature for: □, (−)-eph; ○, (+)-eph. Solid lines were obtained by fitting data points to eq 3. The error bars are inside data points.

were calculated by using viscosity values of pure water at temperature T (η^0) reported elsewhere.[41,42]

From the analysis of the hydrated radii as obtained by the so-called Walden's rule (eq 5), there is a trend for the decrease of r_h with increasing temperature. This deviation from the Walden rule can be justified by alterations of ion−solvent interactions or the cosphere effect upon increasing temperature.[43] The later hypothesis is supported by MDS (see discussion below), once there was no significant difference on the RDFs at two different temperatures (298.15 and 310.15) K; it is also worthy of note that from the comparison of r_h values with RDFs (Figure 2), we may conclude that the transport properties of ephedrine are mainly dependent on the first hydration shell.

The temperature dependence of Λ^0 (Figure 1) can be represented in the framework of the kinetic conductance theory[44,45] by the equation

$$\ln \lambda^0(\text{eph}^+) + \frac{2}{3}\ln d = -\frac{\Delta H^*}{RT} + B \qquad (6)$$

where d is the density of the solvent, R is the gas constant, B is the integration constant, and ΔH^* is the activation enthalpy of the transport process. Figure 1 shows the dependence of the natural logarithm of the molar conductivity at infinitesimal concentration as a function of $1/T$. The values of water density at different temperatures were taken from ref 46. The dependence on the molar conductivity at infinitesimal concentration as a function of $1/T$ follows a linear relationship, according to eq 3, with the following slopes: 2097 (± 60) K and 2318 (± 54) K, for (−)-eph$^+$ and (+)-eph$^+$, respectively. So, the

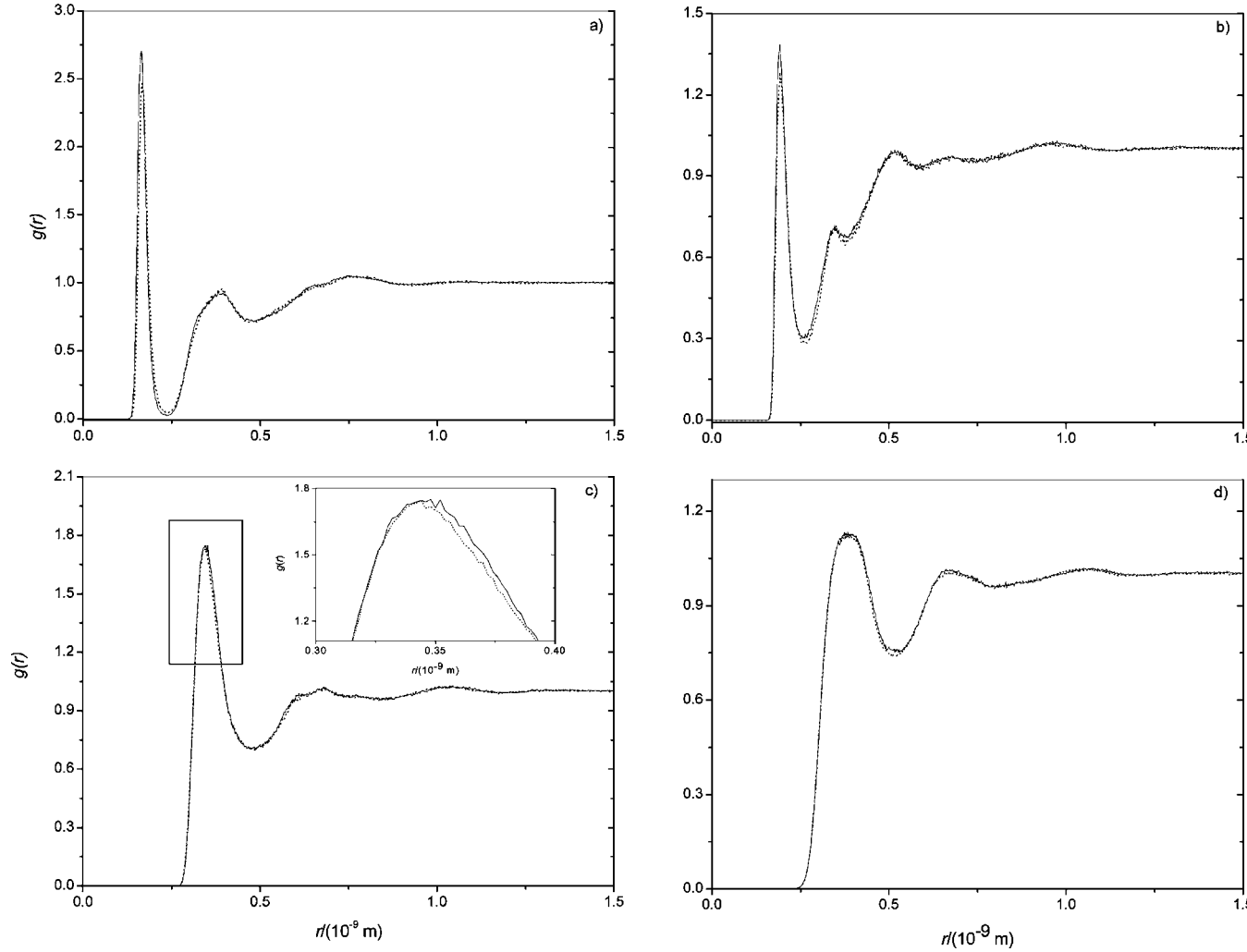

Figure 2. RDF of water oxygen around the H atom of hydroxyl (a) and ammonium (b) groups of ephedrine and water oxygen (c) and hydrogen (d) around one of the carbon atoms of aromatic ring of ephedrine, for (−)-eph (solid lines) and (+)-eph (dotted lines) at 298.15 K. Inset: zoom of the square marked zone on the left.

Table 5. Diffusion Coefficients, D^a, of (1*R*,2*S*)-(−)-Ephedrine Hydrochloride in Aqueous Solutions at Various Concentrations, *c*, at (298.15 and 310.15) K

	T = 298.15 K				T = 310.15 K			
c / mol·dm^{-3}	D^a / 10^{-9}·m^2·s^{-1}	$S_D{}^b$ / 10^{-9}·m^2·s^{-1}	$D'_{OF}{}^c$ / 10^{-9}·m^2·s^{-1}	$\Delta D/D'_{OF}{}^d$ / %	D^a / 10^{-9}·m^2·s^{-1}	$S_{DS}{}^b$ / 10^{-9}·m^2·s^{-1}	$D'_{OF}{}^a$ / 10^{-9}·m^2·s^{-1}	$\Delta D/D''_{OF}{}^b$ / %
0.00125	1.150	0.005	1.126	+2.0	1.570	0.007	1.432	+9.6
0.00250	1.100	0.009	1.118	−1.6	1.560	0.004	1.423	+9.6
0.00499	1.090	0.004	1.113	−2.0	1.501	0.010	1.418	+5.8
0.00746	1.028	0.009	1.111	−7.0	1.445	0.008	1.415	+2.2
0.01000	1.005	0.009	1.108	−9.0	1.408	0.010	1.412	0.0

[a] D is the mean diffusion coefficient for three experiments. [b] S_D is the standard deviation of that mean. [c] Diffusion coefficients of (1*R*,2*S*)-(−)-ephedrine hydrochloride calculated from the Onsager−Fuoss theory [D_{OF}/ (10^{-9}·m^2·s^{-1})] at (298.15 and 310.15) K (eq 12) using a = 21.18 (± 5.98)·10^{-10} m and a = 20.58 (± 4.54)·10^{-10} m, respectively. [d] $\Delta D/D'_{OF}$ and $\Delta D/D''_{OF}$ represent the relative deviations between D (Table 5) and D'_{OF} and D and D''_{OF} values, respectively.

Table 6. Diffusion Coefficients, D^a, of (1*S*,2*R*)-(+)-Ephedrine Hydrochloride in Aqueous Solutions at Various Concentrations, *c*, at (298.15 and 310.15) K

	T = 298.15 K				T = 310.15 K			
c / mol·dm^{-3}	D^a / 10^{-9}·m^2·s^{-1}	$S_D{}^b$ / 10^{-9}·m^2·s^{-1}	$D_{OF}{}^c$ / 10^{-9}·m^2·s^{-1}	$\Delta D/D'_{OF}{}^d$ / %	D^a / 10^{-9}·m^2·s^{-1}	$S_D{}^b$ / 10^{-9}·m^2·s^{-1}	$D_{OF}{}^c$ / 10^{-9}·m^2·s^{-1}	$\Delta D/D''_{OF}{}^d$ / %
0.0010	1.135	0.007	1.100	+3.2	1.567	0.005	1.455	+7.7
0.0025	1.125	0.005	1.094	+3.1	1.530	0.009	1.450	+5.5
0.0050	1.099	0.007	1.086	+1.2	1.480	0.004	1.440	+2.7
0.0080	1.050	0.006	1.083	−3.0	1.420	0.009	1.436	−1.1
0.0100	1.013	0.007	1.081	−6.3	1.379	0.008	1.434	−3.5

[a] D is the mean diffusion coefficient for three experiments. [b] S_D is the standard deviation of that mean. [c] Diffusion coefficients of (1*R*,2*S*)-(−)-ephedrine hydrochloride calculated from the Onsager−Fuoss theory [D_{OF}/ (10^{-9}·m^2·s^{-1})] at (298.15 and 310.15) K (eq 12) using a = 22.08 (± 5.93)·10^{-10} m and a = 23.21 (± 4.98)·10^{-10} m, respectively [d] $\Delta D/D'_{OF}$ and $\Delta D/D''_{OF}$ represent the relative deviations between D (Table 6) and D'_{OF} and D and D''_{OF} values, respectively.

corresponding values for ΔH^* are 17.4 (± 0.5) kJ·mol^{-1} and 19.3 (± 0.4) kJ·mol^{-1}. These enthalpy values are of the same order of magnitude of those reported recently by Bester-Rogac[16] for drugs with similar structures (e.g., sodium salycilate).

However, it should be stressed that there is a slight difference in the activation enthalpy for the ionic migration of (−)- and (+)-ephedrine, showing some discrimination between both enantiomers. The analysis of the activation enthalpies for both enantiomers suggests that (+)-eph has a negative hydration compared with the (−)-eph;[47,48] it means that the migration of water molecules from its hydration sphere to the bulk solution is most difficult.

Although the MDS results (see Section 3.3) for both (−)-eph and (+)-eph isomers are quite similar, some subtle differences arise in the RDFs: (i) the interactions between the water molecules and the hydrophilic part of ephedrine (ammonium and alcohol groups) appear to be slightly stronger for the (−)-eph (the RDFs show a higher peak at smaller distances for the first hydrated shell); (ii) the interactions between the water molecules and the hydrophobic part of ephedrine (aromatic ring) appear to be more significant in the case of (+)-eph (the RDFs show slightly more straight peaks at smaller distances for the first hydrated shell). Since the solvent-exposed surface of the hydrophobic part of ephedrine is clearly larger than the hydrophilic one, it is expected that the differences between the two isomers in (ii) become dominant over those in (i) and, hence, may explain our conductivity data. In light of these results, we believe that the desolvation and rearrangement of ions in the vicinity of ephedrine hydrochloride are mainly controlled by the hydrophobic part of ephedrine structure. Such a hydrophobic effect on the enthalpy activation of charge transport in drugs has been recently pointed out.[16]

3.2. Mutual Diffusion Coefficients. The average diffusion coefficient values, D, for the binary systems water + (−)-eph and water + (+)-eph, at concentrations from (0.001 to 0.01) mol·dm^{-3} for each solute, respectively, at (298.15 and 310.15) K, are summarized in Tables 5 and 6 (with uncertainties of (1 to 2) %). For the purposes of our research, it was not necessary to extend the limits in concentration indicated in Tables 5 and 6.

Table 7. Fitting Coefficients (a_0 to a_2) of the Polynomial Equation [D/(m^2·s^{-1}) = a_0 + a_1 (c/mol·dm^{-3})] to the Mutual Differential Diffusion Coefficients of Ephedrines Hydrochloride in Aqueous Solutions at (298.15 and 310.15) K

	T/K	a_0·10^9	a_1·10^9	R^{2a}
(2*R*,1*S*)-(−)-eph	298.15	1.158	−15.84	0.944
	310.15	1.597	−18.82	0.991
(1*S*,2*R*)-(+)-eph	298.15	1.157	−13.81	0.976
	310.15	1.585	−21.27	0.997

[a] R^2: correlation coefficient.

The concentration dependence of the measured diffusion coefficients can be represented by the linear equation (standard deviation < 1 %)

$$D/(10^{-9}\text{·m}^2\text{·s}^{-1}) = a_0 + a_1 c \qquad (7)$$

where the coefficients a_0 and a_1 are adjustable parameters. The least-squares values of these parameters are listed in Table 7. These may be used to calculate values of diffusion coefficients at specified concentrations within the range of the experimental data shown in Tables 5 and 6. The goodness of the fit (obtained with a confidence interval of 98 %) can be assessed by the excellent correlation coefficients, R^2, and the low percentage of standard deviation (< 1 %). Tables 5 to 8 show the effect of the chirality of ephedrine on the mutual diffusion coefficients of aqueous solutions of ephedrine at 298.15 K, in a concentration range between (1 and 10) mmol·dm^{-3}. Diffusion coefficients of ephedrines decrease by increasing the concentration. It is possible to observe that, increasing the temperature, diffusion data shows some selectivity toward enantiomeric forms of the ephedrine. This is in agreement with electrical conductance data.

To understand this transport process of this electrolyte in aqueous solutions, as a first approach the experimental mutual

Table 8. Comparison of Limiting Diffusion Coefficients of Ephedrine Hydrochloride, as Calculated by the Nernst Equation (Equation 12) and from Conductometric Data, D^0_N, and Those Obtained by Extrapolation of the Diffusion Measurements, D^0_{exp}

T / K	D^0_N [a] / 10^{-9}·m^2·s^{-1}	D^0_{exp} [b] / 10^{-9}·m^2·s^{-1}	$(\Delta D^0/D^0_{exp})$ [c] / %
		(2*R*,1*S*)-(−)-eph	
298.15	1.145	1.158	−1.1
310.15	1.515	1.597	−5.1
		(1*S*,2*R*)-(+)-eph	
298.15	298.15	1.118	1.157
310.15	310.15	1.539	1.585

[a] These values have been calculated with eq 12, using our conductivity data, shown in this table. [b] See Tables 7 and 8. [c] $\Delta D^0/D$ represents the relative deviations between the limiting diffusion coefficients of ephedrine (−) and (+) chloride, respectively, D^0, at 298.15 and 310.15 K, respectively, obtained by eq 12 and from conductivity measurements, and those obtained by extrapolation of the diffusion measurements.

diffusion coefficients at 298.15 K were compared with those estimated using Onsager−Fuoss equation, eq 8 (Tables 5 and 6; see, e.g., ref 38),

$$D = \bar{M}\left(\frac{|z_1| + |z_2|}{|z_1 z_2|}\right)\frac{RT}{c}\left(1 + c\frac{\partial \ln \gamma_{\pm}}{\partial c}\right) \quad (8)$$

where D is the mutual diffusion coefficient of the electrolyte in m^2·s^{-1}, R is the gas constant in J·mol^{-1}·K^{-1}, T is the absolute temperature, z_1 and z_2 are the algebraic valences of a cation and of an anion, respectively, and the last term in parentheses is the activity factor, with $y_{\pm}$ being the mean molar activity coefficient, c the concentration in mol·m^{-3}, and $\bar{M}$, in mol^2·s·m^{-3}·kg^{-1}, given by

$$\bar{M} = \frac{1}{N_A^2 e_0^2}\left(\frac{\lambda_1^0\lambda_2^0}{\nu_2|z_2|\lambda_1^0 + \nu_1|z_1|\lambda_2^0}\right)c + \Delta\bar{M}' + \Delta\bar{M}'' \quad (9)$$

In eq 9, the first-and second-order electrophoretic terms are given by

$$\Delta\bar{M}' = -\frac{c}{N_A} = \frac{(|z_2|\lambda_1^0 - |z_1|\lambda_2^0)^2}{(|z_1|\nu_1\lambda_2^0 + |z_2|\nu_2\lambda_1^0)^2}\frac{\nu_1\nu_2}{\nu_1 + \nu_2}\frac{k}{6\pi\eta_0(1 + ka)} \quad (10)$$

and

$$\Delta\bar{M}'' = \frac{(\nu_1|z_2|\lambda_1^0 + \nu_2|z_1|\lambda_2^0)^2}{(\nu_1|z_1|\lambda_2^0 + \nu_2|z_2|\lambda_1^0)^2}\frac{1}{(\nu_1 + \nu_2)^2}\frac{1}{N_A{}^2}\frac{k^4\varphi(ka)}{48\pi^2\eta_0} \quad (11)$$

where η_0 is the viscosity of the water in N·s·m^{-2}, N_A is the Avogadro's constant, e_0 is the proton charge in coulombs, ν_1 and ν_2 are the stoichiometric coefficients, λ_1^0 and λ_2^0 are the limiting molar conductivities of the cation and anion, respectively, in m^2·mol^{-1}·Ω^{-1}, k is the "reciprocal average radius of ionic atmosphere" in m^{-1}, a is the mean distance of closest approach of ions in m, $\phi(ka) = |e^{2ka}E_i(2ka)/(1 + ka)|$ has been tabulated by Harned and Owen, and the other letters represent well-known quantities.[38] In this equation, phenomena such as complexation and/or ion association[37] and hydrolysis[49,50] are not taken into consideration. There is no direct method for measuring the ion size parameter a, the "mean distance of closest approach" from the Debye−Huckel theory, but it may be estimated from MDS; the following values of a have been computed: for (1*R*,2*S*)-(−)-ephedrine hydrochloride $a = 21.18\ (\pm 5.98)\cdot 10^{-10}$ m and $a = 20.58\ (\pm 4.54)\cdot 10^{-10}$ m and for (1*S*,2*R*)-(+)-ephedrine hydrochloride, $a = 22.08\ (\pm 5.93)\cdot 10^{-10}$ m and $a = 23.21\ (\pm 4.98)\cdot 10^{-10}$ m, for (298.15 and 310.15) K, respectively.

Comparing the calculated diffusion coefficients of these electrolytes, D_{OF} (Table 5 and 6), using the values of the parameter a obtained from MDS, with the related experimental values at 298.15 K, a reasonable agreement is observed between the experimental data and this model for both systems at dilute solutions (deviations, in general, ≤ 3 % for $c < 0.07$ M). Having in mind that those deviations are approximately the same order as the experimental uncertainties (usually within ± (2 to 3) %) and that the phenomena as association is not contemplated in the Onsager−Fuoss equation, we can interpret that the predominant species responsible for the behavior of D for this range of concentration are ephedrine ions and chloride ions. Moreover, the acceptable deviations (ca. < 3 %) between the limiting D^0 value calculated by extrapolating experimental data to $c \rightarrow 0$ (Tables 7 and 8) and the Nernst values (eq 12) and from conductivity measurements are another evidence.

$$D^0 = \frac{RT}{F^2}\frac{|Z_+| + |Z_-|}{|Z_+Z_-|}\frac{\lambda_+^0\lambda_-^0}{\lambda_+^0|Z_-| + \lambda_-^0|Z_+|} \quad (12)$$

Z_+ and Z_- represent the algebraic valences of a cation and an anion, respectively. λ_-^0 and λ_+^0 are the molar conductance at infinitesimal concentration of chloride and ephedrine, respectively.

The decrease of the diffusion coefficient, when the concentration increases, may be attributed to the nonideality in thermodynamic behavior which is allowed for by the factor $(1 + c\ \mathrm{d}\ln y/\mathrm{d}\ln c)$ (eq 8).[37] Their interpretation can be made on the basis of new species resulting from the eventual formation of ion pairs or higher aggregates of these salts, assuming that those species have a lower mobility than the ephedrine and chloride (Figure 1) because of its size (though an estimate of their amounts is not possible). We may assume that there are also other species in lower proportions, but they do not influence significantly the behavior of the diffusion of this system.

For $c > 0.007$ mol·dm^{-3}, the results predicted from the above model differ from experimental observation by (3 to 9) %. This is not surprising since we take into account the change with concentration of parameters such as viscosity, dielectric constant, and above all, hydration,[37] which are not taken into account in the Onsager−Fuoss model.

In relation to the effect of temperature on diffusion, an increase in the experimental D values was found at all ephedrine chloride concentrations. Also, the decrease of the diffusion coefficient was obtained when the concentration increases. Also, the acceptable deviation between the limiting D^0 value calculated by extrapolating experimental data to $c \rightarrow 0$ (Tables 7 and 8) and the Nernst values (Table 8) (deviations ≤ 5 %) were verified. Despite the absence of the values of parameters for estimations of D_{OF} for this temperature, the agreement between the calculated diffusion coefficients of these electrolytes, D_{OF} (Tables 5 and 6), and the related experimental values is also reasonable (that is, deviations ≤ 9 %). However, at this temperature, for both systems and for the interval $0.005\ \mathrm{M} < c \leq 0.01$ M, the deviations among these diffusion coefficients are not too significant, contrarily to the results observed at 298.15 K. Such a result would seem to indicate that the solute−solute interactions (which can result in the aggregate stabilization) are enhanced because of the thermal effect. This effect can contribute to the decrease of these interactions and, consequently, may be responsible for no significant difference among theoretical and experimental of diffusion coefficients

3.3. Simulations. The structure of the ephedrine solution can be analyzed from the RDFs shown in Figures 2 and S1 of Supporting Information. In Figures 2 and S1, the RDF of the water oxygen around the hydrogen of the alcohol group in ephedrine, at (298.15 and 310.15) K, respectively, is shown. It is apparent from Figure 2a that, for both (1*R*,2*S*)-(−)- and (1*S*,2*R*)-(+)-ephedrine isomers, the RDF presents a thin peak at $1.6 \cdot 10^{-10}$ m, which is associated with the strong alcohol−water hydrogen bond. Though broader, the prominent peak arising at $3.8 \cdot 10^{-10}$ m may correspond to a second shell of water molecules in the neighborhood of the alcohol group. A very small third peak can be visualized at longer distances ($\sim 7.7 \cdot 10^{-10}$ m); eventually, this is a consequence of the long-range perturbation in the structure of water due to the presence of the alcohol group.

Looking at the RDF of the water oxygen around one of the hydrogens in the ephedrine ammonium group (Figure 2b), it is possible to observe a narrow peak at $1.9 \cdot 10^{-10}$ m for both isomers, which again can be assigned to a slightly longer hydrogen bond. Indeed, the calculated average number of ephedrine−water hydrogen bonds is around three, which can be related with both of the two hydrogens in the ammonium group and the hydrogen of the alcohol group. As a general trend, the increase of temperature does not significantly change the intensity of the peaks (especially the first one), while a slightly higher peak for (1*R*,2*S*)-(−)-ephedrine indicates a stronger hydrogen bond, which shows a smaller average number of hydrogen bonds (n) for (1*S*,2*R*)-(+)-ephedrine ((−)-eph: $n_{298} = 3.18$ and $n_{310} = 3.17$; (+)-eph: $n_{298} = 3.00$ and $n_{310} = 3.00$).

To complete the analysis of the structural properties of ephedrine in water, we show the radial distribution of water oxygens around one of the carbons in the aromatic ring in Figure 2c. In this case, the maximum of probability occurs for $3.4 \cdot 10^{-10}$ m, which is about twice the length found in Figures 2a,b for a hydrogen bond. Although not shown, small peaks at similar distances are found for the RDF of the water oxygen around the corresponding hydrogen of the aromatic ring. This clearly indicates that the interaction solvent ephedrine (from the ring side) is of hydrophobic-type (i.e., dominated by long-range van der Waals forces). In addition, very small peaks appear in Figure 2c at $6.8 \cdot 10^{-10}$ m and $10 \cdot 10^{-10}$ m.

Further insight about the structure of the solvent around the aromatic ring can be extracted from Figure 2d, which shows the RDF of the water hydrogens around the same carbon as in Figure 2c. It is worth noting in Figure 2d that the peaks in the RDF appear approximately at the same positions as in Figure 2c, which indicates that water molecules are oriented preferentially tangential to the plan of the aromatic ring. A similar behavior has been found for the hydrophobic hydration of methane.[51]

4. Conclusions

We have measured the electrical conductivity and diffusion coefficients of two ephedrine enantiomers, (1*S*,2*R*)-(+)-ephedrine hydrochloride and (1*R*,2*S*)-(−)-ephedrine hydrochloride, in aqueous solutions. We have complemented these studies with MDS's. The dependence of electrical conductivity on the temperature, ranging from (298.15 to 323.15) K, shows that the limiting ionic conductivity of the cationic (1*S*,2*R*)-(+)-ephedrine has higher values at higher temperatures, leading to a small differentiation in the activation enthalpies of the transport process: 19.3 (± 0.4) kJ·mol^{-1} and 7.4 (± 0.5) kJ·mol^{-1} for (1*S*,2*R*)-(+)-ephedrine and (1*R*,2*S*)-(−)-ephedrine, respectively. In a previous report (refs 52−55), the origins of enantiodifferentiation with ephedrine and α-cyclodextrin were assigned to the configuration *a* to the amino group. The (2*R*)-(+)-enantiomer was the more strongly bound, and in the (2*S*)-(−)-complex it was proposed that there was an unfavorable steric interaction between the 2-Me group and the H3 proton of the cyclodextrin host that inhibited a favorable NH···O hydrogen bonding interaction. Such discrimination has also been detected by dynamic molecular simulations; however, it should be worthy to conclude that the role of the hydrophobic hydration, of ephedrine, cannot also be neglected and even can have an important effect on the transport properties.

Although no conclusions on the enantiomer's discrimination can be taken from the analysis of mutual diffusion coefficients for ephedrine at the studied concentrations, extrapolated diffusion coefficients at a differential concentration for (1*R*,2*S*)-(−)- and (1*S*,2*R*)-(+)-ephedrine hydrochloride show a good agreement with Nernst diffusion coefficients derived from conductance data. From the latter, the estimated values of diffusion coefficients for these electrolytes are ($1.145 \cdot 10^{-9}$ and $1.118 \cdot 10^{-9}$) m^2·s^{-1} at 298.15 K, respectively, and ($1.515 \cdot 10^{-9}$ and $1.539 \cdot 10^{-9}$) m^2·s^{-1} at 310.15 K, respectively; from diffusion, we obtained ($1.158 \cdot 10^{-9}$ and $1.157 \cdot 10^{-9}$) m^2·s^{-1} at 298.15 K, respectively, and ($1.597 \cdot 10^{-9}$ and $1.585 \cdot 10^{-9}$) m^2·s^{-1} at 310.15 K, respectively.

We believe that these experimental data will contribute for a better knowledge of ephedrine enantiomers in aqueous solutions and thus help to better understand the mechanism behind enantiodifferentiation.

Supporting Information Available:

RDF of water oxygen around the H atom of hydroxyl and ammonium groups of ephedrine and water oxygen and hydrogen around one of the carbon atoms of aromatic ring of ephedrine, for (−)-eph and (+)-eph at 310.15 K. This material is available free of charge via the Internet at http://pubs.acs.org.

Literature Cited

(1) Gmeiner, G.; Geinsendorfer, T.; Kainzbauer, J.; Nikolajevic, M. In *Recent Advances in Doping Analysis*; Donik, M., Schänzer, W., Gotzmann, A., Mareck-Engelke, U., Eds.; Sports and Buch Strauss: Köln, Germany, 2001; Vol. 9.

(2) Shekelle, P. G.; Hardy, M. L.; Morton, S. C.; Maglione, M.; Mojica, W. A.; Suttorp, M. J.; Rhodes, S. L.; Jungvig, L.; Gagne, J. Efficacy and safety of ephedra and ephedrine for weight loss and athletic performance - A meta-analysis. *JAMA, J. Am. Med. Assoc.* **2003**, *289*, 1537–1545.

(3) Zhang, L.; Han, D. M.; Song, X. H.; Wang, H.; Wang, K. J.; Liu, Z. Y. Effects of ephedrine on human nasal ciliary beat frequency. *ORL* **2008**, *70*, 91–96.

(4) Vansal, S. S.; Feller, D. R. Direct effects of ephedrine isomers on human beta-adrenergic receptor subtypes. *Biochem. Pharmacol.* **1999**, *58*, 807–810.

(5) Ranieri, T. L.; Ciolino, L. A. Rapid selective screening and determination of ephedrine alkaloids using GC-MS footnote mark. *Phytochem. Anal.* **2008**, *19*, 127–135.

(6) Porto, R. M. D.; Perez, A. R.; Vidal, M. T. C.; Fraga, M. G. Qualitative confirmation procedure for ephedrines as acetonide derivatives in doping urine samples by gas chromatography/electron ionization mass spectrometry. *Rapid Commun. Mass Spectrom.* **2009**, *23*, 249–257.

(7) Deventer, K.; Pozo, O. J.; Van Eenoo, P.; Delbeke, F. T. Development and validation of an LC-MS/MS method for the quantification of ephedrines in urine. *J. Chromatogr., B* **2009**, *877*, 369–374.

(8) Rekharsky, M. V.; Goldberg, R. N.; Schwarz, F. P.; Tewari, Y. B.; Ross, P. D.; Yamashoji, Y.; Inoue, Y. Thermodynamic and nuclear-magnetic-resonance study of the interactions of alpha-cyclodextrin and beta-acyclodextrin with model substances - phenethylamine, ephedrines, and related substances. *J. Am. Chem. Soc.* **1995**, *117*, 8830–8840.

(9) Kataky, R.; Parker, D.; Kelly, P. M. Potentiometric, enantioselective sensors for alkyl and aryl ammonium-ions of pharmaceutical significance, based on lipophilic cyclodextrins. *Scand. J. Clin. Lab. Invest.* **1995**, *55*, 409–419.

(10) Gafni, A.; Cohen, Y.; Kataky, R.; Palmer, S.; Parker, D. Enantiomer discrimination using lipophilic cyclodextrins studied by electrode response, pulsed-gradient spin-echo (PGSE) NMR and relaxation rate measurements. *J. Chem. Soc., Perkin Trans. 2* **1998**, 19–23.
(11) Kataky, R.; Lopes, P. Chiral detection at a liquid-liquid interface. *Chem. Commun.* **2009**, 1490–1492.
(12) Piletsky, S. A.; Karim, K.; Piletska, E. V.; Day, C. J.; Freebairn, K. W.; Legge, C.; Turner, A. P. F. Recognition of ephedrine enantiomers by molecularly imprinted polymers designed using a computational approach. *Analyst* **2001**, *126*, 1826–1830.
(13) Ansell, R. J.; Wang, D. Y.; Kuah, J. K. L. Imprinted polymers for chiral resolution of (±)-ephedrine. Part 2: probing pre-polymerisation equilibria in different solvents by NMR. *Analyst* **2008**, *133*, 1673–1683.
(14) Yu, Z.; Cui, M.; Yan, C. Y.; Song, F. R.; Liu, Z. Q.; Liu, S. Y.; Zhang, G.; Zhang, H. X. Gas-phase chiral discrimination of ephedrine and pseudoephedrine associated with cyclodextrins. *J. Mass Spectrom.* **2007**, *42*, 1106–1110.
(15) Hu, X. B.; Li, G. T.; Li, M. H.; Huang, J.; Li, Y.; Gao, Y. B.; Zhang, Y. H. Ultrasensitive specific stimulant assay based on molecularly imprinted photonic hydrogels. *Adv. Funct. Mater.* **2008**, *18*, 575–583.
(16) Bester-Rogac, M. Nonsteroidal Anti-Inflammatory Drugs Ion Mobility: A Conductometric Study of Salicylate, Naproxen, Diclofenac and Ibuprofen Dilute Aqueous Solutions. *Acta Chim. Slov.* **2009**, *56*, 70–77.
(17) Bester-Rogac, M.; Boncina, M.; Apelblat, Y.; Apelblat, A. Electrical conductances of dilute aqueous solutions of sodium penicillin G, potassium penicillin G, and potassium penicillin V in the 278.15−313.15 K temperature range. *J. Phys. Chem. B* **2007**, *111*, 11957–11967.
(18) Ribeiro, A. C. F.; Santos, C.; Lobo, V. M. M.; Cabral, A.; Veiga, F. J. B.; Esteso, M. A. Diffusion Coefficients of the Ternary System beta-Cyclodextrin plus Caffeine + Water at 298.15 K. *J. Chem. Eng. Data* **2009**, *54*, 115–117.
(19) Merclin, N.; Beronius, P. Transport properties and association behaviour of the zwitterionic drug 5-aminolevulinic acid in water-A precision conductometric study. *Eur. J. Pharm. Sci.* **2004**, *21*, 347–350.
(20) Ribeiro, A. C. F.; Valente, A. J. M.; Lobo, V. M. M.; Azevedo, E. F. G.; Amado, A. M.; da Costa, A. M. A.; Ramos, M. L.; Burrows, H. D. Interactions of vanadates with carbohydrates in aqueous solutions. *J. Mol. Struct.* **2004**, *703*, 93–101.
(21) Barthel, J.; Feuerlein, F.; Neueder, R.; Wachter, R. Calibration of conductance cells at various temperatures. *J. Sol. Chem.* **1980**, *9*, 209–219.
(22) Valente, A. J. M.; Burrows, H. D.; Pereira, R. F.; Ribeiro, A. C. F.; Pereira, J.; Lobo, V. M. M. Effect of Europium(III) chloride on the aggregation behavior of sodium dodecyl sulfate. *Langmuir* **2006**, *22*, 5625–5629.
(23) Lobo, V. M. M.; Valente, A. J. M.; Ribeiro, A. C. F. Differential mutual diffusion coefficients of electrolytes measured by an open-ended conductimetric capillary cell: a review. In *Focus on chemistry and biochemistry*; Zaikov, G. E., Lobo, V. M. M., Guarrotxena, N., Eds.; Nova Science Publications|: New York, 2003.
(24) Ribeiro, A. C. F.; Lobo, V. M. M.; Azevedo, E. F. G.; Miguel, M. D.; Burrows, H. D. Diffusion coefficients of sodium dodecylsulfate in aqueous solutions of sucrose and in aqueous solutions. *J. Mol. Liq.* **2001**, *94*, 193–201.
(25) Ribeiro, A. C. F.; Lobo, V. M. M.; Azevedo, E. F. G.; Miguel, M. D.; Burrows, H. D. Diffusion coefficients of sodium dodecylsulfate in aqueous solutions and in aqueous solutions of beta-cyclodextrin. *J. Mol. Liq.* **2003**, *102*, 285–292.
(26) Valente, A. J. M.; Ribeiro, A. C. F.; Lobo, V. M. M.; Jimenez, A. Diffusion coefficients of lead (II) nitrate in nitric acid aqueous solutions at 298 K. *J. Mol. Liq.* **2004**, *111*, 33–38.
(27) Ribeiro, A. C. F.; Barros, M. C. F.; Teles, A. S. N.; Valente, A. J. M.; Lobo, V. M. M.; Sobral, A.; Esteso, M. A. Diffusion coefficients and electrical conductivities for calcium chloride aqueous solutions at 298.15 and 310.15 K. *Electrochim. Acta* **2008**, *54*, 192–196.
(28) Hess, B.; Kutzner, C.; van der Spoel, D.; Lindahl, E. GROMACS 4: Algorithms for highly efficient, load-balanced, and scalable molecular simulation. *J. Chem. Theory Comput.* **2008**, *4*, 435–447.
(29) Wang, J. M.; Wolf, R. M.; Caldwell, J. W.; Kollman, P. A.; Case, D. A. Development and testing of a general amber force field. *J. Comput. Chem.* **2004**, *25*, 1157–1174.
(30) Cornell, W. D.; Cieplak, P.; Bayly, C. I.; Gould, I. R.; Merz, K. M.; Ferguson, D. M.; Spellmeyer, D. C.; Fox, T.; Caldwell, J. W.; Kollman, P. A. A 2nd generation force-field for the simulation of proteins, nucleic-acids, and organic-molecules. *J. Am. Chem. Soc.* **1995**, *117*, 5179–5197.
(31) Wang, J. M.; Cieplak, P.; Kollman, P. A. How well does a restrained electrostatic potential (RESP) model perform in calculating conformational energies of organic and biological molecules. *J. Comput. Chem.* **2000**, *21*, 1049–1074.
(32) Weiner, S. J.; Kollman, P. A.; Case, D. A.; Singh, U. C.; Ghio, C.; Alagona, G.; Profeta, S.; Weiner, P. A new force-field for molecular mechanical simulation of nucleic-acids and proteins. *J. Am. Chem. Soc.* **1984**, *106*, 765–784.
(33) Weiner, S. J.; Kollman, P. A.; Nguyen, D. T.; Case, D. A. An all atom force-field for simulations of proteins and nucleic-acids. *J. Comput. Chem.* **1986**, *7*, 230–252.
(34) Berendsen, H. J. C.; Grigera, J. R.; Straatsma, T. P. The missing term in effective pair potentials. *J. Phys. Chem.* **1987**, *91*, 6269–6271.
(35) Kusalik, P. G.; Svishchev, I. M. The spatial structure in liquid water. *Science* **1994**, *265*, 1219–1221.
(36) Evans, D. J.; Holian, B. L. The Nose-Hoover thermostat. *J. Chem. Phys.* **1985**, *83*, 4069–4074.
(37) Robinson, R. A.; Stokes, R. H. *Electrolyte solutions*; Dover Publications, Inc.: New York, 2002.
(38) Harned, H. S.; Owen, B. B. *The physical chemistry of electrolytic solutions*; Reinhold Publications Co.: New York, 1967.
(39) Vlaev, L.; Georgieva, V. Temperature and concentration dependence of the electrical conductance, diffusion, and kinetics parameters of the ions in aqueous solutions of sulfuric acid, selenic acid, and potassium tellurate. *J. Solution Chem.* **2005**, *34*, 961–980.
(40) Barthel, J.; Krienke, H.; Kunz, W. *Physical chemistry of electrolyte solutions: modern aspects*; Springer: New York, 1996.
(41) Korson, L.; Drosthan, W.; Millero, F. J. Viscosity of water at various temperatures. *J. Phys. Chem.* **1969**, *73*, 34–39.
(42) Bester-Rogac, M. Determination of the limiting conductances and the ion-association constants of calcium and manganese sulfates in water from electrical conductivity measurements. *Acta Chim. Slov.* **2008**, *55*, 201–208.
(43) Smedley, S. I. *The interpretation of ionic conductivity in liquids*; Plenum Press: New York, 1980.
(44) Brummer, S. B.; Hills, G. J. Kinetics of ionic conductance. 1. Energies of activation and constant volume principle. *Trans. Faraday Soc.* **1961**, *57*, 1816–1822.
(45) Tsurko, E. N.; Neueder, R.; Barthel, J. Electrolyte conductivity of NaSCN in propan-1-ol and propan-2-ol solutions at temperatures from 228 to 298 K. *J. Chem. Eng. Data* **2000**, *45*, 678–681.
(46) Rodriguez, H.; Brennecke, J. F. Temperature and composition dependence of the density and viscosity of binary mixtures of water plus ionic liquid. *J. Chem. Eng. Data* **2006**, *51*, 2145–2155.
(47) Marcus, Y. Effect of Ions on the Structure of Water: Structure Making and Breaking. *Chem. Rev.* **2009**, *109*, 1346–1370.
(48) Samoilov, O. Y. A new approach to the study of hydration of ions in aqueous solutions. *Discuss. Faraday Soc.* **1957**, 141–146.
(49) Baes, C. F. J.; Mesmer, R. E. *The hydrolysis of cations*; John Wiley & Sons: New York, 1976.
(50) Burguess, J. *Metal ions in solution*; John Wiley & Sons: Chichester, Sussex, England, 1978.
(51) Hernandez-Cobos, J.; Mackie, A. D.; Vega, L. F. The hydrophobic hydration of methane as a function of temperature from histogram reweighting Monte Carlo simulations. *J. Chem. Phys.* **2001**, *114*, 7527–7535.
(52) Amato, M. E.; Lombardo, G. M.; Pappalardo, G. C.; Scarlata, G. High-field NMR techniques, molecular modeling and molecular-dynamics simulations in the study of the inclusion complex of the cognition activator (±)−1-(4-methoxybenzoyl)-5-oxo-2-pyrrolidinepropanoic acid (CI-933) with beta-cyclodextrin. *J. Mol. Struct.* **1995**, *350*, 71–82.
(53) Black, D. R.; Parker, C. G.; Zimmerman, S. S.; Lee, M. L. Enantioselective binding of alpha-pinene and of some cyclohexanetriol derivatives by cyclodextrin hosts: A molecular modeling study. *J. Comput. Chem.* **1996**, *17*, 931–939.
(54) Eliseev, A. V.; Iacobucci, G. A.; Khanjin, N. A.; Menger, F. M. Enantioselective folding at the cyclodextrin surface. *J. Chem. Soc. Chem. Commun.* **1994**, 2051–2052.
(55) Kohler, J. E. H.; Hohla, M.; Richters, M.; Konig, W. A. A molecular-dynamic simulation of the complex-formation between methyl (R)/(S)-2-chloropropionate and heptakis(3-o-acetyl-2,6-di-o-pentyl)-beta-cyclodextrin. *Chem. Ber.* **1994**, *127*, 119–126.

Received for review July 8, 2009. Accepted August 26, 2009. Financial support from Acção Integrada Luso-Britânica (B-1/08 and B-48/09) is gratefully acknowledged.

JE9005757